JOC Article
pubs.acs.org/joc

On the Mechanism of Cyclization of 5-Hexenylchromate Intermediates in the Reactions of Fischer Carbene Complexes with a Lithium Enolate and Allylmagnesium Bromide

Pablo Campomanes,[†,§] Josefa Flórez,[‡] Iván Pérez-Sánchez,[‡] Marcos G. Suero,[‡] Tomás L. Sordo,[†] and M. Isabel Menéndez*[,†]

[†]*Departamento de Química Física y Analítica and* [‡]*Instituto Universitario de Química Organometálica "Enrique Moles", Unidad Asociada al CSIC, Universidad de Oviedo, C/Julián Clavería 8, 33006 Oviedo, Spain.* [§]*Present address: Laboratory of Computational Chemistry and Biochemistry, École Polytechnique Fédérale de Lausanne (EPFL), CH-1015 Lausanne, Switzerland*

isabel@uniovi.es

Received June 25, 2009

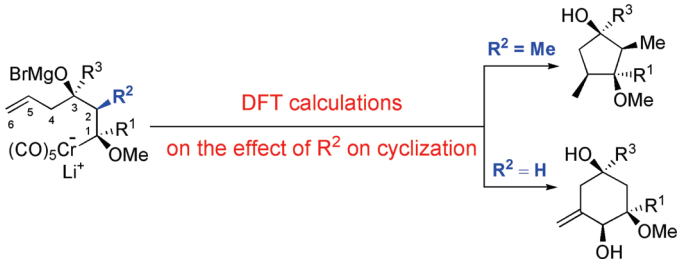

The mechanisms for the evolution of pentacarbonyl-5-hexenylchromate complexes, unsubstituted and methyl substituted at C2, formed from a pentacarbonyl(alkoxy)carbene complex of chromium, the corresponding ketone lithium enolate, and allylmagnesium bromide, were theoretically investigated by using DFT (Density Functional Theory) at the B3PW91/6-31G* level (LANL2DZ for Cr and Br) taking into account the effect of THF solvent through the PCM model (Polarizable Continuum Model). Methyl substitution at C2 provokes a shortening of about 5° in the C1−C2−C3 angle that favors the formation of the pentacyclic product. Also, the presence of this methyl substituent at C2 sterically disfavors the formation of the hexacyclic product. Thus, our results yield the hexacyclic system as the most favored product for the evolution of the unsubstituted alkylpentacarbonylchromate complex, and the pentacyclic product in the case of the substituted system, in good agreement with the experimental findings. The stereochemistry of the products experimentally observed is determined at the transition state for the migration of the $Cr(CO)_5$ fragment from C1 to C6 and the conformational rearrangement of the C1−C6 skeleton. Amine molecules, present in the reaction medium, can play a catalytic role by assisting the 1,2-H migration in the last step for the formation of hexacyclic products.

Introduction

Transition metal-mediated multicomponent reactions are powerful synthetic tools that allow the rapid elaboration of complex structures. These processes are particularly attractive for their application in both target-oriented and diversity-oriented synthesis and in the context of combinatorial chemistry.[1−3] Fischer carbene complexes are well-recognized as very versatile reagents in many useful multicomponent methodologies.[4,5] These organometallics very often allow incorporation of carbonyl ligands in the final molecule in addition to the carbene ligand.

(1) *Multicomponent Reactions*; Zhu, J., Bienaymé, H., Eds.; Wiley-VCH: Weinheim, Germany, 2005.
(2) Orru, R. V. A.; de Greef, M. *Synthesis* **2003**, 1471–1499.
(3) Mihovilovic, M. D.; Stanetty, P. *Angew. Chem., Int. Ed.* **2007**, *46*, 3612–3615.
(4) *Metal Carbenes in Organic Synthesis*; Topics in Organometallic Chemistry, Vol. 13; Dötz, K. H., Ed.; Springer-Verlag: Berlin, Germany, 2004.
(5) Barluenga, J.; Fernández-Rodríguez, M. A.; Aguilar, E. *J. Organomet. Chem.* **2005**, *690*, 539–587.

DOI: 10.1021/jo901353s Published on Web 08/18/2009

SCHEME 1. Cyclization Reactions with Ketone Lithium Enolates

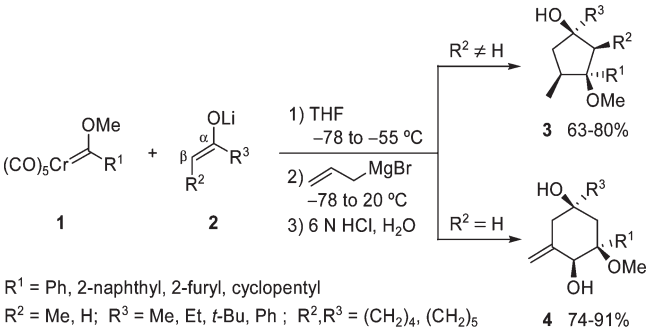

SCHEME 2. Cyclization Reactions with Ester Lithium Enolates

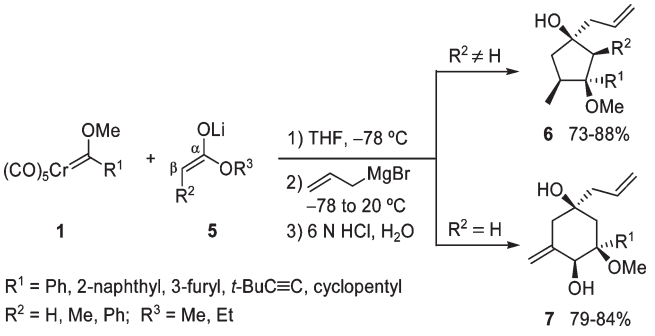

In this context we have found that the successive reaction at low temperature of a pentacarbonyl(alkoxy)carbene complex of chromium **1** with a ketone or ester lithium enolate **2** or **5** and then with allylmagnesium bromide afforded diastereoselectively and after hydrolysis at room temperature, either pentasubstituted cyclopentanols **3**/**6** or tetrasubstituted 1,4-cyclohexanediols **4**/**7** depending mainly on the degree of substitution at the Cβ position of the enolate anion (Schemes 1 and 2).[6,7] Lithium enolates **2**/**5** substituted at the Cβ position ($R^2 \neq H$) led selectively to the five-membered carbocycles when combined with carbene complexes **1** (R^1 = Ph, 2-naphthyl, 2-furyl, cyclopentyl), while the six-membered-ring derivatives were selectively formed in the experiments with enolates **2**/**5** unsubstituted at the Cβ atom (R^2 = H) and carbene complexes **1** (R^1 = Ph, 2-naphthyl, 3-furyl, 3,3-dimethyl-1-butynyl, cyclopentyl). However, some exceptions have been found in particular reactions performed with 2-naphthylcarbene complex **1** (R^1 = 2-naphthyl) and ketone lithium enolates **2** (R^2 = H, R^3 = Me, *t*-Bu) and with alkynylcarbene complex **1** (R^1 = 3,3-dimethyl-1-butynyl) and methyl propionate lithium enolate **5** ($R^2 = R^3$ = Me).[7] These highly functionalized carbocycles **3**, **4**, **6**, and **7** are new structural elements that provide cyclopentane and cyclo hexane derivatives with novel substitution patterns.

To explain the formation of these cyclic derivatives we have initially proposed a reaction mechanism outlined in Scheme 3 that involves addition of the lithium enolate **2**/**5** to

SCHEME 3. Initial Mechanistic Proposal for the Formation of Compounds 3, 4, 6, and 7

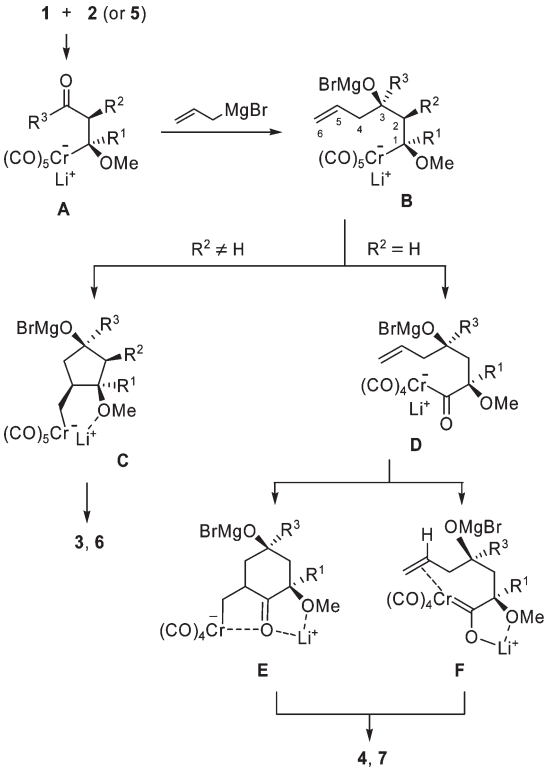

the carbene carbon atom of complex **1** and subsequent addition of the Grignard reagent to the carbonyl group of intermediate **A**.[6,7] Alkylpentacarbonylchromate intermediates **B** substituted at C2 ($R^2 \neq H$) presumably adopt a more folded chain conformation[8] that facilitates the intramolecular carbometalation reaction to give cyclopentylmethylchromate derivatives **C** and after hydrolysis cyclopentanols **3**/**6**. On the other hand, intermediates **B** that do not have a substituent at C2 (R^2 = H) would undergo faster a migratory insertion of carbon monoxide presumably as a consequence of a more extended chain conformation. Cyclization of acyltetracarbonylchromate species **D** to finally furnish upon protonation 1,4-cyclohexanediols **4**/**7** could occur through an intramolecular formal insertion of the carbene carbon atom into the secondary vinylic C−H bond of the allyl group (intermediate **F**) or alternatively through an intramolecular alkene-insertion reaction to give intermediates **E**.

To better understand the mechanism of this kind of highly selective multicomponent cyclizations we have theoretically investigated the evolution of pentacarbonyl-5-hexenylchromate complexes **B** (R^1 = Ph; R^2 = H, Me; R^3 = Me) formed from pentacarbonyl(1-methoxybenzylidene)chromium **1** (R^1 = Ph), acetone or 2-butanone lithium enolate **2** (R^2 = H, Me; R^3 = Me), and allylmagnesium bromide to yield in each case the corresponding pentasubstituted cyclopentanols, **3**, and the tetrasubstituted 1,4-cyclohexanediols, **4**.

(6) Barluenga, J.; Pérez-Sánchez, I.; Rubio, E.; Flórez, J. *Angew. Chem., Int. Ed.* **2003**, *42*, 5860–5863.

(7) Barluenga, J.; Pérez-Sánchez, I.; Suero, M. G.; Rubio, E.; Flórez, J. *Chem.—Eur. J.* **2006**, *12*, 7225–7235.

(8) Increasing alkyl substitution on an open chain is known to facilitate the cyclization processes: (a) Sammes, P. G.; Weller, D. J. *Synthesis* **1995**, 1205–1222. (b) Pawlowski, M.; Maurin, J. K.; Leniewski, A.; Wojtasiewicz, K.; Czarnocki, Z. *Heterocycles* **2005**, *65*, 9–22.

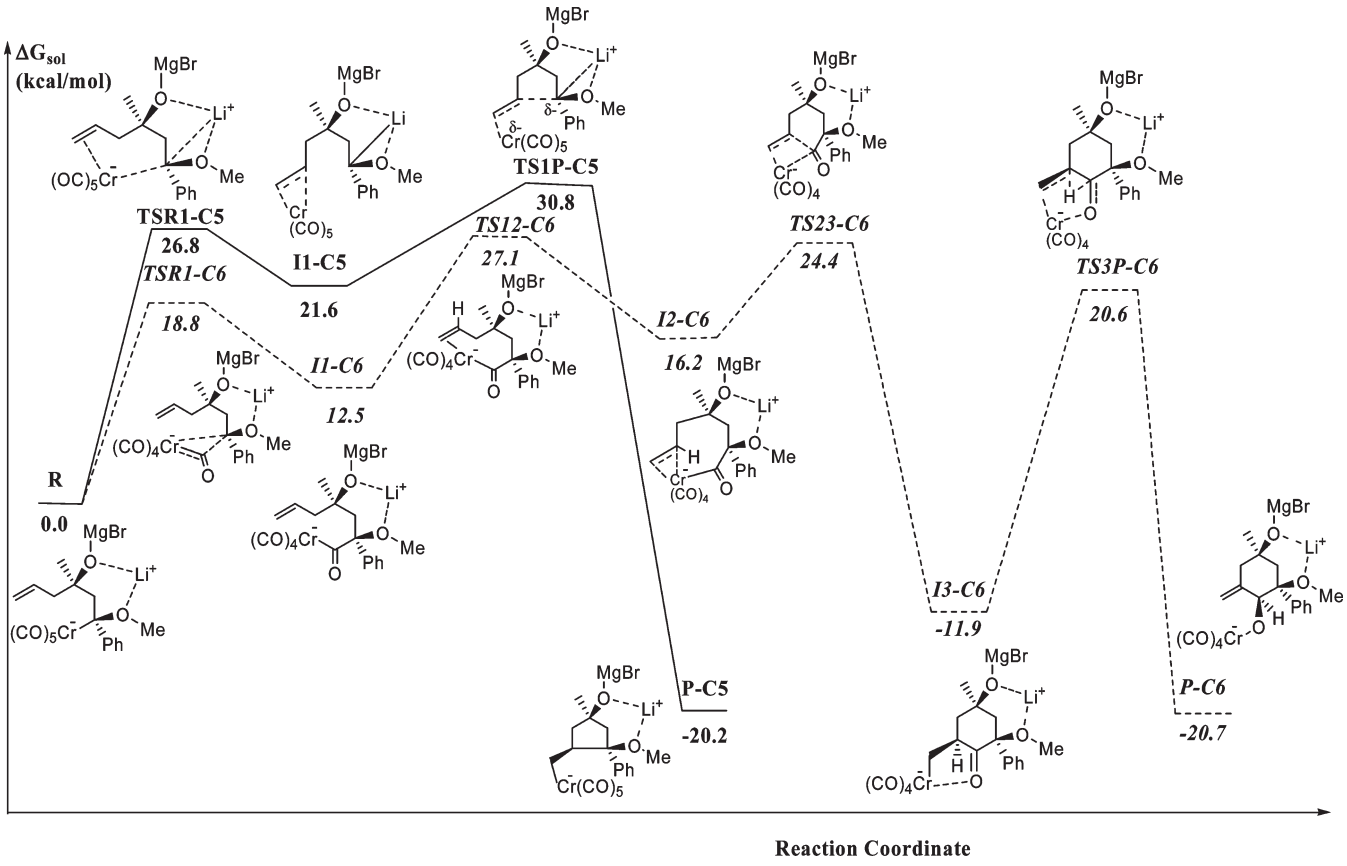

FIGURE 1. Gibbs energy profile for the reactions from 2-unsubstituted 5-hexenylchromate complex, **R**, to yield the 5-membered cyclic product **P-C5** and the hexacyclic product **P-C6**.

Computational Methods

Full geometry optimizations were performed with B3LYP and B3PW91 density functional theory (DFT) methods,[9−11] using the relativistic effective core pseudopotential LANL2DZ[12] for Cr and Br, and the 6-31G* basis set for the remaining atoms. All calculations were carried out with the Gaussian 03 series of programs.[13] The nature of the stationary points located was further checked and zero point vibrational energies (ZPVE) were evaluated by analytical computations of harmonic vibrational frequencies at the same theory level. Intrinsic reaction coordinate (IRC) calculations were also carried out with the B3LYP functional to check the connection between the transition states (TSs) and the minimum energy structures by using the Gonzalez and Schlegel method[14,15] implemented in Gaussian 03.

ΔG_{gas} values were also calculated within the ideal gas, rigid rotor, and harmonic oscillator approximations.[16] A pressure of 1 atm and a temperature of 298.15 K were assumed in the calculations.

To take into account solvent effects we used a Self-Consistent-Reaction-Field (SCRF) model proposed for quantum chemical computations on solvated molecules.[17−20] The solvent is represented by a dielectric continuum characterized by its relative static dielectric permittivity ε. The solute, which is placed in a cavity created in the continuum after spending some cavitation energy, polarizes the continuum, which in turn creates an electric field inside the cavity. This interaction can be taken into account using quantum chemical methods by minimizing the electronic energy of the solute plus the Gibbs energy change corresponding to the solvation process.[21] Addition to ΔG_{gas} of the solvation Gibbs energy gives $\Delta G_{solution}$.

(9) Becke, A. B. *J. Chem. Phys.* **1993**, *98*, 5648–5662.
(10) Becke, A. B. *Phys. Rev. A* **1988**, *38*, 3098–3100.
(11) Lee, C.; Yang, W.; Parr, R. G. *Phys. Rev. B* **1988**, *37*, 785–789.
(12) Hay, P. J.; Wadt, W. R. *J. Chem. Phys.* **1985**, *82*, 299–310.
(13) Frisch, M. J.; Trucks, G. W.; Schlegel, H. B.; Scuseria, G. E.; Robb, M. A.; Cheeseman, J. R.; Montgomery, J. A., Jr.; Vreven, T.; Kudin, K. N.; Burant, J. C.; Millam, J. M.; Iyengar, S. S.; Tomasi, J.; Barone, V.; Mennucci, B.; Cossi, M.; Scalmani, G.; Rega, N.; Petersson, G. A.; Nakatsuji, H.; Hada, M.; Ehara, M.; Toyota, K.; Fukuda, R.; Hasegawa, J.; Ishida, M.; Nakajima, T.; Honda, Y.; Kitao, O.; Nakai, H.; Klene, M.; Li, X.; Knox, J. E.; Hratchian, H. P.; Cross, J. B.; Bakken, V.; Adamo, C.; Jaramillo, J.; Gomperts, R.; Stratmann, R. E.; Yazyev, O.; Austin, A. J.; Cammi, R.; Pomelli, C.; Ochterski, J. W.; Ayala, P. Y.; Morokuma, K.; Voth, G. A.; Salvador, P.; Dannenberg, J. J.; Zakrzewski, V. G.; Dapprich, S.; Daniels, A. D.; Strain, M. C.; Farkas, O.; Malick, D. K.; Rabuck, A. D.; Raghavachari, K.; Foresman, J. B.; Ortiz, J. V.; Cui, Q.; Baboul, A. G.; Clifford, S.; Cioslowski, J.; Stefanov, B. B.; Liu, G.; Liashenko, A.; Piskorz, P.; Komaromi, I.; Martin, R. L.; Fox, D. J.; Keith, T.; Al-Laham, M. A.; Peng, C. Y.; Nanayakkara, A.; Challacombe, M.; Gill, P. M. W.; Johnson, B.; Chen, W.; Wong, M. W.; Gonzalez, C.; Pople, J. A. *Gaussian 03*, Revision B.04; Gaussian, Inc., Wallingford, CT, 2004.
(14) Gonzalez, C.; Schlegel, H. B. *J. Chem. Phys.* **1989**, *90*, 2154–2161.
(15) Gonzalez, C.; Schlegel, H. B. *J. Phys. Chem.* **1990**, *84*, 5523–5527.
(16) McQuarrie, D. A. *Statistical Mechanics*; Harper & Row: New York, 1986.
(17) Rivail, J. L.; Rinaldi, D.; Ruiz-López, M. F. In *Theoretical and Computational Model for Organic Chemistry*; Formosinho, S. J., Csizmadia, I. G., Arnaut, L., Eds.; NATO ASI Series C; Kluwer Academic Publishers: Dordrecht, The Netherlands, 1991.
(18) Cramer, C. J.; Truhlar, D. G. In *Reviews in Computational Chemistry*; Lipkowitz, K. B., Boyd, D. B., Eds.; VCH: New York, 1995.
(19) Rivail, J. L.; Rinaldi, D. In *Computational Chemistry: Review of Current Trends*; Leszczynski, J., Ed.; World Scientific: New York, 1995.
(20) Cramer, C. J.; Truhlar, D. G. *Chem. Rev.* **1999**, *99*, 2161–2200.
(21) Claverie, P. In *Quantum Theory of Chemical Reactions*; Daudel, R., Pullman, A., Salem, L., Veillard, A., Eds.; Reidel: Dordrecht, The Netherlands, 1982.

Within the different approaches which can be followed to calculate the electrostatic potential created by the polarized continuum in the cavity we have employed the Polarizable Continuum Model (PCM)[22,23] with the united atom Hartree−Fock (UAHF) parametrization.[24] The solvation Gibbs energies $\Delta G_{solvation}$ along the reaction coordinate were evaluated from single-point PCM calculations on the gas phase optimized geometries at the same theory level. A relative permittivity of 7.58 was employed to simulate THF as the solvent used in the experimental work.

Results and Discussion

Although the optimized geometries obtained with B3LYP and B3PW91 functionals are very similar, the corresponding electronic and Gibbs energies present quite remarkable differences. As the B3PW91 energies are in much better agreement with experimental findings we will only present and discuss in the text the corresponding Gibbs energy profiles in solution. To simulate the coordination of solvent molecules (THF) to Mg and Li atoms we have explicitly added three molecules of dimethyl ether to the reactive system, one coordinated to the lithium atom and two to the magnesium atom.

Evolution of the 2-Unsubstituted 5-Hexenylchromate Complex R. Figures 1 and 2 and Table 1S of the Supporting Information display the B3PW91 results obtained for the evolution of the 2-unsubstituted 5-hexenylchromate complex **R** (**B**: R^1 = Ph, R^2 = H, R^3 = Me). At this complex lithium atom is coordinated to the methoxy O atom (1.900 Å), to the O atom bonded to C3 (1.874 Å), and to the oxygen of one molecule of dimethyl ether (1.987 Å), while its distance to C1 is 2.562 Å. This coordination of the lithium atom to those three oxygen atoms is found in all the structures along the reaction paths studied by us.

According to our theoretical calculations the 2-unsubstituted 5-hexenylchromate complex can evolve through the transition state (TS) **TSR1-C5** (26.8 kcal/mol) for the migration of $Cr(CO)_5$ from C1 to C6 and the conformational rearrangement of the C1−C6 carbon skeleton through rotation about C5−C4 and C4−C3 axes to form the intermediate **I1-C5** (21.6 kcal/mol). At **TSR1-C5** the Li atom starts a bonding interaction with C1 (2.152 Å), which is reinforced at **I1-C5** (2.115 Å) due to the breaking of the bond between C1 and Cr. At **I1-C5** the C1−C5 distance is 3.215 Å so that this conformation is adequate to undertake cyclization (see Figures 1 and 2). The intermediate **I1-C5** evolves through the TS **TS1P-C5** (30.8 kcal/mol) for C1−C5 bonding to give the 5-membered cyclic product **P-C5** (−20.2 kcal/mol). At **TS1P-C5** the Li atom, still coordinated to the two oxygen atoms of the system and to the oxygen atom of one molecule of dimethyl ether, goes away from C1 to a distance of 2.426 Å. On the other hand, we found a second pathway for the evolution of 2-unsubstituted 5-hexenylchromate complex **R** through the TS **TSR1-C6** (18.8 kcal/mol) for the insertion of one of the CO ligands of $Cr(CO)_5$ into the C1−Cr bond to form the intermediate **I1-C6** (12.5 kcal/mol). This intermediate undertakes a conformational rearrangement of the C1−C6 carbon skeleton through rotation about C5−C4 and C4−C3 axes to prepare (C1)−CO−C5 bonding with simultaneous migration of Cr from (C1)−CO to C6 through the TS **TS12-C6** (27.1 kcal/mol) to yield the intermediate **I2-C6** (16.2 kcal/mol), which, in turn, evolves to the TS **TS23-C6** (24.4 kcal/mol) to form the hexacyclic intermediate **I3-C6** (−11.9 kcal/mol). Finally, this cyclic intermediate undergoes a 1,2-H shift with simultaneous migration of Cr from C6 to the O atom of the inserted C═O, through the TS **TS3P-C6** (20.6 kcal/mol), to render the hexacyclic product **P-C6** (−20.7 kcal/mol). The C5−C6 bond length varies from 1.530 Å at **I3-C6** to 1.341 Å at **P-C6**, clearly indicating the formation of a double bond between C5 and C6. It must be noted that although the energy barrier for this last step **I3-C6** f **TS3P-C6** is high (32.5 kcal/mol) that corresponding to the backward process **I3-C6** → TS23-C6 (36.3 kcal/mol) is even greater by 3.8 kcal/mol.

Given that the rate determinant TS for the formation of the 5-membered-ring derivative, **TS1P-C5**, is higher in energy than the rate determinant TS for the formation of the 6-membered-ring compound, **TS12-C6**, by 3.7 kcal/mol our theoretical results predict that the only product obtained from the 2-unsubstituted 5-hexenylchromate complex **R** would be the hexacyclic derivative **P-C6** in agreement with the experimental results.

It must be remarked that after extensive search we have not found any viable path for the evolution of acylchromate complex **I1-C6** through an intramolecular formal insertion of the carbene carbon atom (C of the inserted CO) into the secondary vinylic C−H bond of the allyl group (C5-H).

Evolution of the 2-Methyl Substituted 5-Hexenylchromate Complex R′. Figures 3 and 4 and Table 2S of the Supporting Information display the B3PW91 results obtained for the evolution of the 2-methyl-5-hexenylchromate complex **R′** (**B**: R^1 = Ph, R^2 = R^3 = Me). In this complex the lithium atom is coordinated to the methoxy O atom (1.889 Å), to the O atom bonded to C3 (1.868 Å), and to the oxygen of one molecule of dimethyl ether (1.990 Å), while its distance to C1 is 2.573 Å. Again, this coordination of the lithium atom to those three oxygen atoms remains all along the reaction paths.

As in the case of the unsubstituted complex we found that the 2-methyl-substituted 5-hexenylchromate complex **R′** can evolve along an analogous mechanistic pathway through **TSR1′-C5** (19.4 kcal/mol; C1−Li = 2.759 Å), **I1′-C5** (12.0 kcal/mol; C1−Li = 2.133 Å), and **TS1P′-C5** (19.7 kcal/mol; C1−Li = 2.353 Å) to yield the corresponding 5-membered-ring product **P′-C5** (−34.2 kcal/mol; C1−Li = 2.942 Å). The rate determinant step in this cyclization process is also the formation of the C1−C5 bond (**TS1P′-C5**). The lithium atom approaches C1 after the chromium atom has migrated from it at **I1′-C5** and moves away from C1 when this carbon atom starts interacting with C5 to form the pentacyclic product.

Similarly, the substituted complex **R′** can evolve along the mechanistic route **TSR1′-C6** (13.0 kcal/mol), **I1′-C6** (4.2 kcal/mol), **TS12′-C6** (22.3 kcal/mol), **I2′-C6** (6.8 kcal/mol), and **TS23′-C6** (14.8 kcal/mol) to form a 6-membered cyclic intermediate, **I3′-C6** (−24.0 kcal/mol), which yields the final product **P′-C6** (−30.6 kcal/mol) after a 1,2-H shift through the TS **TS3P′-C6** (9.7 kcal/mol). As in the unsubstituted system, the energy barrier from **I3′-C6** backward to **I2′-C6**

(22) Tomasi, J.; Persico, M. *Chem. Rev.* **1994**, *94*, 2027–2094.
(23) Tomasi, J.; Cammi, R. *J. Comput. Chem.* **1996**, *16*, 1449–1458.
(24) Barone, V.; Cossi, M.; Tomasi, J. *J. Chem. Phys.* **1997**, *107*, 3210–3221.

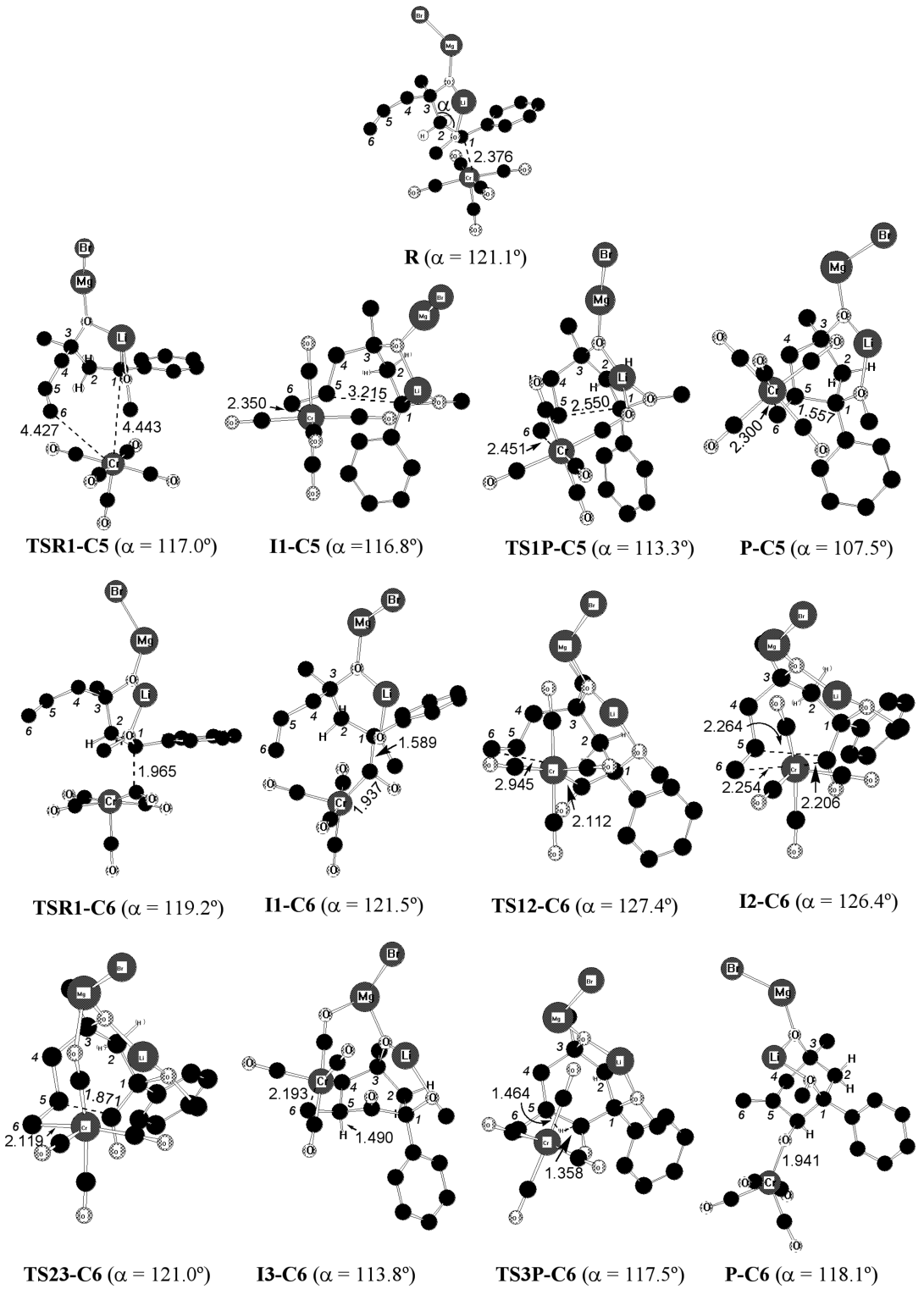

FIGURE 2. B3PW91 optimized structures (without nonrelevant H atoms) for the reactions from 2-unsubstituted 5-hexenylchromate complex, **R**, to yield the 5-membered cyclic product **P-C5** and the hexacyclic product **P-C6** (α is the C1−C2−C3 angle).

(38.8 kcal/mol) is 5.1 kcal/mol greater than that for the evolution from **I3′-C6** to form the final product **P′-C6** (33.7 kcal/mol).

The rate determining step for the formation of the 6-membered cycle corresponds to the conformational rearrangement and Cr migration, **TS12′-C6**, which presents a Gibbs energy barrier 2.6 kcal/mol higher than that of **TS1P′-C5** for the formation of the pentacyclic product **P′-C5**. Then, according to our results, the only product expected from the evolution of the 2-substituted 5-hexenylchromate complex **R′** would be the 5-membered cycle, in agreement with the experimental results.

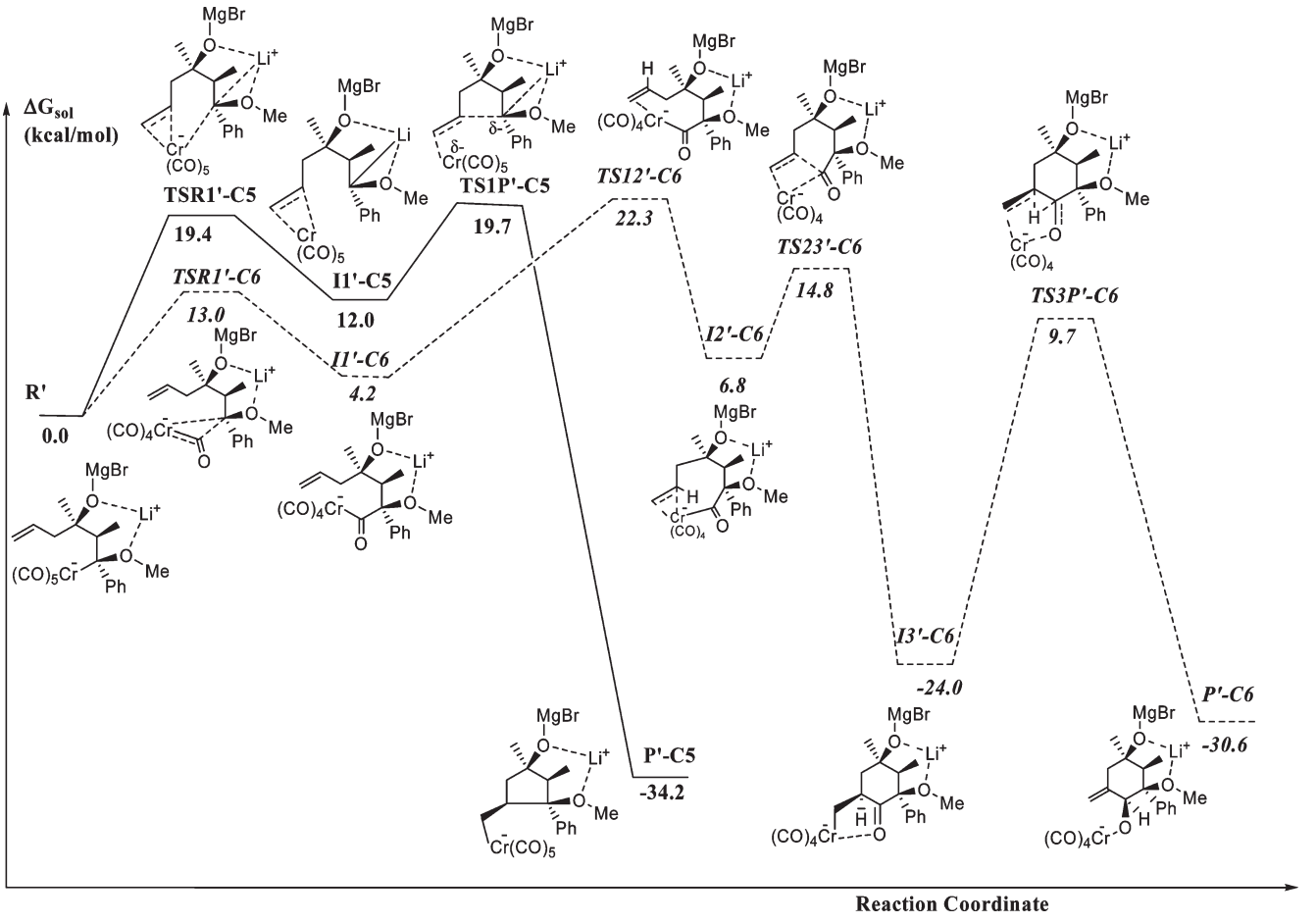

FIGURE 3. Gibbs energy profile for the reactions from 2-methyl substituted 5-hexenylchromate complex, **R′**, to yield the 5-membered cyclic product **P′-C5** and the hexacyclic product **P′-C6**.

Again, no viable mechanistic path has been found for the evolution of acylchromate complex **I1′-C6** through an intramolecular formal insertion of the carbene carbon atom (C of the inserted CO) into the secondary vinylic C5−H bond of the allyl group.

Discussion. Comparing Figures 1 and 3 it is clear that the presence of the methyl substituent at C2 causes an important stabilization of all the species located along the pentaannulation (*C5*) and hexaannulation (*C6*) pathways with respect to the reactant. From Figures 2 and 4 we see that the presence of the methyl substituent at C2 provokes a decrease in the C1−C2−C3 angle (α angle) in the range of 1−5°. This structural change clearly favors the formation of the C1−C5 bond to form the 5-membered cycle along the *C5* route. If we compare the variation of the Gibbs energy in solution when going from **I1-C5** to **TS1P-C5** (9.2 kcal/mol) with that when going from **I1′-C5** to **TS1P′-C5** (7.7 kcal/mol) we can quantify this effect in about 1.5 kcal/mol. On the other hand, the methyl substituent at C2 also presents a steric interaction with the phenyl group and with the methyl group on C3, which is more important at **TS12′-C6** than at **I1′-C6** since these groups are closer to each other at the transition states. Assuming that the difference between the variation of the Gibbs energy in solution when going from **I1-C6** to **TS12-C6** (14.6 kcal/mol) and that when going from **I1′-C6** to **TS12′-C6** (18.1 kcal/mol) is mainly due to the steric effect of the methyl substituent we can quantify this effect as about 3.5 kcal/mol. As the structure effect favors **TS1P′-C5** and the steric effect disfavors **TS12′-C6** these two effects would explain the inversion of relative stability of **TS1P-C5** and **TS12-C6** when introducing the methyl substituent at C2. This would explain the change in the product obtained experimentally.

We found that the diisopropylamine experimentally present in the reaction medium can play an important catalytic role in the evolution of **I3-C6** and **I3′-C6**. In effect, the amine, modeled in our calculations by a dimethylamine molecule, reduces the energy barrier corresponding to **TS3P-C6** and **TS3P′-C6** by about 5 and 7 kcal/mol, respectively, acting as a shuttle for the migrating H atom (see Figure 5 and Table 3S of the Supporting Information).

It is interesting to remark that the stereochemistry of the last stereogenic center formed in the pentacyclization step to yield the cyclopentylmethylchromate, **P-C5** and **P′-C5**, is determined by the rearrangement taking place when the electrophilic chromium atom approaches the C5−C6 double bond at **TSR1-C5** and **TSR1′-C5**. In effect, at **TS1P-C5** and **TS1P′-C5** C1 attacks C5 from the same face of the C=C double bond where the chromium atom is located. Analogously, the stereochemistry of the stereogenic center C5 at **I3-C6** and **I3′-C6** is

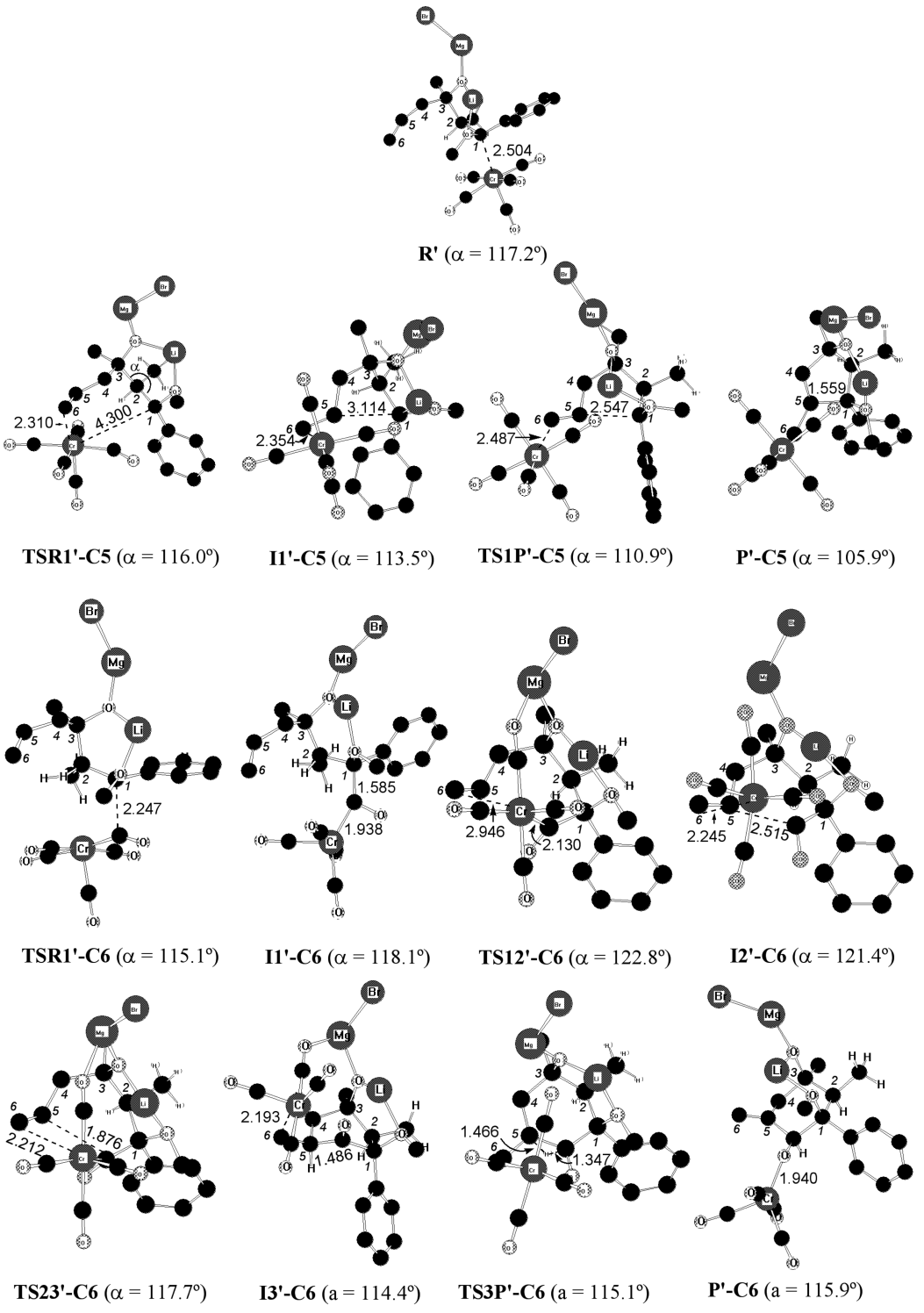

FIGURE 4. B3PW91 optimized structures (without nonrelevant H atoms) for the reactions from 2-methyl substituted 5-hexenylchromate complex, **R′**, to yield the 5-membered cyclic product **P′-C5** and the hexacyclic product **P′-C6** (α is the C1−C2−C3 angle).

determined by the coordination of the electrophilic chromium atom to the C5−C6 double bond at **TS12-C6** and **TS12′-C6**.

At **TS3P-C6** and **TS3P′-C6** the migrations of the H atom on C5 to the C atom of the inserted CO and of the chromium atom from C6 to the carbonyl O take place. The result of this 1,2-H shift is in agreement with the stereochemistry experimentally observed. At **I3-C6** and **I3′-C6** C6, C5, and C=O are nearly in the same plane (dihedral angle −17.8° and −16.6°, respectively); the H and Cr atoms are placed on opposite faces of this plane and each undergoes migration over its corresponding face. When the amine molecule assists the 1,2-H shift the migrating H atom follows an analogous route.

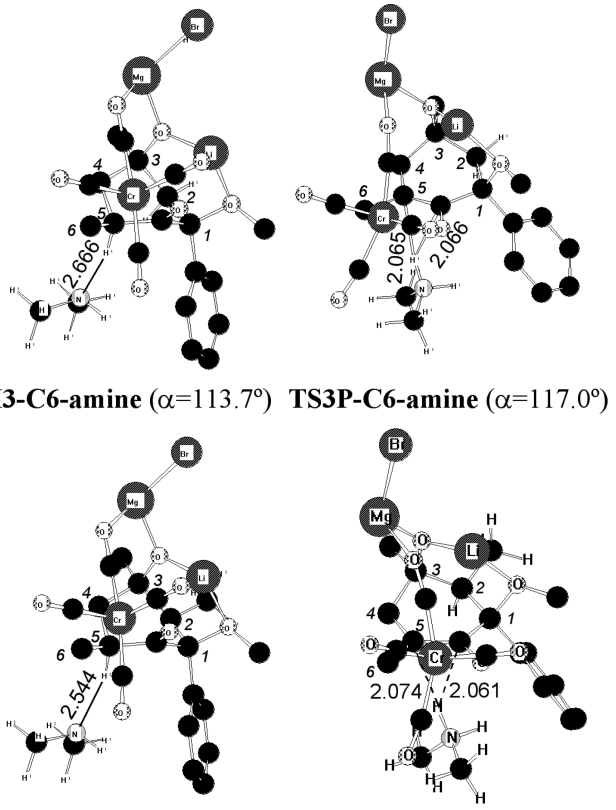

I3-C6-amine (α=113.7°) **TS3P-C6-amine** (α=117.0°)

I3'-C6-amine (α=111.2°) **TS3P'-C6-amine** (α=114.7°)

FIGURE 5. B3PW91 optimized structures (without nonrelevant H atoms) for the amine catalyzed 1,2 H-shift reaction step to yield the hexacyclic products **P-C6** and **P′-C6**.

Conclusions

The kind of product obtained in the evolution of pentacarbonyl-5-hexenylchromate complexes depends on the substitution at C2. Methyl substitution at this position (C2) produces a more folded conformation, which structurally favors the formation of the pentacyclic product and at the same time disfavors the formation of the hexacyclic product by steric interactions. As a consequence, our results render the hexacyclic system as the most favored product for the evolution of the unsubstituted alkylpentacarbonylchromate complex, and the pentacyclic product in the case of the C2 substituted system, in good agreement with the experimental findings. According to our calculations the stereochemistry of the cyclization products is established at the transition states for migration of the $Cr(CO)_5$ fragment from C1 to C6 and the conformational rearrangement of the C1−C6 skeleton. The lithium atom, which all along the reaction paths is coordinated to the two sp^3 O atoms of the molecule and to the O atom of a dimethyl ether molecule, bonds to C1 when the Cr migrates from it. The last step in the formation of hexacyclic products, corresponding to the 1,2-H shift, can be catalyzed by the assistance of an amine molecule present in the reaction medium, which acts as a shuttle for H migration. We are currently studying cyclizations of analogous intermediates with different substitution patterns.

Acknowledgment. Financial support for this work from the MEC (Spain) (Grant CTQ2007-61048/BQU) is gratefully acknowledged.

Supporting Information Available: Absolute and relative electronic (including ZPVE) and Gibbs energies (both in the gas phase and in solution), full drawings of the optimized structures located in the reaction paths explored in this work (Figures 2S, 4S, and 5S corresponding to Figures 2, 4, and 5, respectively), and the Cartesian coordinates of all these optimized structures. This material is available free of charge via the Internet at http://pubs.acs.org.